LncRNA MIAT stimulates oxidative stress in the hypoxic pulmonary hypertension model by sponging miR-29a-5p and inhibiting Nrf2 pathway

W.-W. LI1, A.-H. CAO2, F.-Y. SUN3

Wenwu Li and Aihua Cao contributed equally to this work

Abstract. – OBJECTIVE: To elucidate the potential biological functions of long non-coding RNA (IncRNA) MIAT in the development of hypoxic pulmonary hypertension (HPH) and the underlying mechanism.

MATERIALS AND METHODS: Twenty Sprague Dawley (SD) rats were randomly assigned into normoxia group (n=10) and hypoxia group (n=10), respectively. *In vivo* HPH model in rats was established by hypoxic induction. Expression levels of MIAT and miR-29a-5p in rats were detected. Meanwhile, hemodynamic indicators in rats were examined. *In vitro* HPH model was conducted in hypoxia-induced HPAECs. The interaction between MIAT and miR-29a-5p was assessed by Dual-Luciferase reporter assay. Moreover, their regulatory effects on viability, migratory ability, oxidative stress, and the Nrf2 pathway in hypoxia-induced HPAECs were examined.

RESULTS: MIAT was upregulated in both *in vivo* and *in vitro* HPH models, while miR-29a-5p was downregulated. Knockdown of MIAT suppressed viability, migratory ability, and oxidative stress in hypoxia-induced HPAECs. MiR-29a-5p was the target gene binding MIAT, and silence of miR-29a-5p partially relieved the inhibitory effects of MIAT on the above regulations in HPAECs.

CONCLUSIONS: MIAT promotes proliferative and migratory abilities, as well as oxidative stress in hypoxia-induced HPAECs by targeting miR-29a-5p, thus aggravating the development of HPH.

Key Words:

LncRNA MIAT, MiR-29a-5p, Hypoxia, Oxidative stress, HPH.

Abbreviations

HPH= hypoxic pulmonary hypertension; HPAECs, human pulmonary artery endothelial cells; ncRNAs =

non-coding RNAs; GWAS = genome-wide association study; SD = sprague dawley; mPAP = mean pulmonary artery pressure; RVSP = right ventricular systolic pressure; PASP = pulmonary artery systolic pressure; RVHI = right ventricular hypertrophy index; RV = right ventricular free wall; LV+S = left ventricle with interventricular septum; SDS-PAGE = sodium dodecyl sulphate-polyacrylamide gel electrophoresis; PVDF = polyvinylidene difluoride; SPSS = statistical product and service solutions.

Introduction

Hypoxic pulmonary hypertension (HPH) is resulted from pulmonary vasoconstriction, remodeling, and thrombosis because of persistent hypoxia, eventually leading to hemodynamic abnormalities and even the right heart failure^{1,2}. The pathogenesis of HPH is complicated, involving multiple signaling transductions and vascular effectors^{3,4}. During the development of HPH, human pulmonary artery endothelial cells (HPAECs) exert a vital role^{5,6}. Hyperplasia, migration, and dedifferentiation of HPAECs contribute to hypertrophy and thickening of the pulmonary vascular wall, thereafter leading to elevated pressure and resistance on the pulmonary artery. Cellular functions of HPAECs are closely linked to inflammation and immunity. Once they are disrupted, pathological changes in the pulmonary artery are irreversibly developed6-8.

Non-coding RNAs (ncRNAs) have been well concerned due to their diverse functions in the human body⁹⁻¹¹. They could be classified into

¹Emergency Department, Hainan People's Hospital, Haikou, China

²Department of Emergency, Shanxian Central Hospital, Heze, China

³Department of Intensive Care Unit, Shanxian Central Hospital, Heze, China

piRNAs, miRNAs, gRNAs, and lncRNAs^{9,11}. Genome-wide association study (GWAS) proposed that over 98% transcripts are ncRNAs in mammals, and less than 2% transcripts are proteins^{12,13}. LncRNAs are ncRNAs with over 200 nt long and they could not encode proteins^{14,15}. LncRNAs exert multi-level regulations and participate in disease progression^{16,17}. Previous studies^{18,19} have demonstrated the critical involvement of lncRNA MIAT during the development of HPH. In this paper, the specific binding between MIAT and miR-29a-5p was predicted by bioinformatics. We established both in vivo and in vitro HPH models and explored the role of MIAT in influencing HPH development.

Materials and Methods

Experimental Animals

A total of 20 male Sprague Dawley (SD) rats weighing 180-220 g (BRL Medicine, Shanghai) were randomly assigned into normoxia group (n=10) and hypoxia group (n=10). Rats in hypoxia group were exposed to 10% O₂ for at least 8 h per day, and HPH model was established 4 weeks later. Rats in both groups were free to drink and eat. This investigation was approved by the Animal Ethics Committee of Shanxian Central Hospital Animal Center.

Hemodynamic Measurements

After weighing, rats were anesthetized by intraperitoneal injection of 4.8% avertin (8 mL/ kg) and fixed on the table. After exposure of suprasternal fossa, the right jugular artery and vein were separated. A 1% heparin-irrigated polyethylene catheter, which was connected to a pressure transducer and multipurpose polygraph, was gently and slowly inserted into the pulmonary artery through the right carotid artery and right ventricle. Right ventricular wave and pulmonary artery wave were recorded. Meanwhile, the mean pulmonary artery pressure (mPAP), right ventricular systolic pressure (RVSP), and pulmonary artery systolic pressure (PASP) were recorded as well. The whole procedure should be quickly completed. Notably, heparin sodium injection should be less injected after the measurement; otherwise, it may cause inaccurate cardiac output because of excessive cardiac preload, and even animal death.

Right Ventricular Hypertrophy Index (RVHI) Determination

The right ventricular free wall (RV), and left ventricle with interventricular septum (LV+S) of the rat were separated and weighed. RVHI=RV/(LV+S).

Biochemical Measurements

Rat pulmonary tissues were collected and immediately stored at liquid nitrogen. Tissue homogenate was subjected to determination of MDA, T-AOC, CAT, GSH, SOD, and ROS activities using relative commercial kits (Jiancheng, Nanjing, China).

Cell Culture

HPAECs and human renal epithelial cell lines (293T) were provided by American Type Culture Collection (ATCC; Manassas, VA, USA). Cells were cultured in Dulbecco's Modified Eagle's Medium (DMEM; Gibco, Rockville, MD, USA) containing 10% fetal bovine serum (FBS; Gibco, Rockville, MD, USA), 100 U/mL penicillin and 100 μg/mL streptomycin in a 5% CO₂ incubator at 37°C. Cell passage was conducted in 1×tryp-sin+ethylenediaminetetraacetic acid (EDTA) at 80-90% confluence.

Transfection and Hypoxic Treatment

Sh-NC and sh-MIAT were provided by Gene-Pharma (Shanghai, China). Cells were inoculated in a 6-well plate and cultured to 30-40% confluence. Cells were transfected with corresponding plasmids (GenePharma, Shanghai, China) using Lipofectamine 2000 (Invitrogen, Carlsbad, CA, USA). Transfected cells for 48 h were harvested for functional experiments. For hypoxic induction, HPAECs were incubated at 37°C and exposed to 1% O₂ and 5% CO₂.

Cell Proliferation Assay

Cells were inoculated in a 96-well plate with 2×10^3 cells per well. At the appointed time points, absorbance value at 490 nm of each sample was recorded using the cell counting kit-8 (CCK-8) kit (Dojindo Laboratories, Kumamoto, Japan) for plotting the viability curves.

Transwell Migration Assay

Cells were inoculated in a 24-well plate with $5.0\times10^5/\text{mL}$. 200 μL of suspension was applied in the upper side of transwell chamber (Millipore, Billerica, MA, USA) inserted in a 24-well plate. In the bottom side, 500 μL of medium

containing 10% FBS was applied. After 48 h of incubation, cells migrated to the bottom side were fixed in methanol for 15 min, dyed with crystal violet for 20 min and counted using a microscope. Migratory cell number was counted in 5 randomly selected fields per sample (magnification 20×).

Ouantitative Real Time-Polymerase Chain Reaction (qRT-PCR)

RNA in cells or tissues was isolated using TRIzol reagent (Invitrogen, Carlsbad, CA, USA). Extracted RNAs were purified by DNase I treatment, and reversely transcribed into complementary deoxyribose nucleic acid (cDNA) using PrimeScript RT Reagent (TaKaRa, Otsu, Shiga, Japan). The obtained cDNA underwent qRT-PCR using SYBR®Premix Ex TaqTM (Ta-KaRa, Otsu, Shiga, Japan). Glyceraldehyde 3-phosphate dehydrogenase (GAPDH) used as internal reference. Each sample was performed in triplicate, and relative level was calculated by 2-\Delta \text{LncRNA MIAT: forward:} 5'-GAGATTGGCGATGGTTGTGA-3', reverse: 5'-CAGTGACGCTCCTTTGTTGAA-3'; tin: forward: 5'-CCTGGCACCCAGCACAAT-3', 5'-TGCCGTAGGTGTCCCTTTG-3'; reverse: forward: 5'-GCGGCGGACTmiR-29a-5p: GATTTCTTTTGGT-3', reverse: 5'-ATCCAGT-GCAGGGTCCGAGG-3'; U6: forward: 5'-GC-CCTCTGTGCTACTTACTC-3', reverse: 5'-GCT-GGTTGTGGGTTACTCTC-3'.

Western Blot

Total protein was extracted from cells or tissues. The obtained protein was separated by sodium dodecyl sulphate-polyacrylamide gel electrophoresis (SDS-PAGE), transferred to polyvinylidene difluoride (PVDF) membranes (Millipore, Billerica, MA, USA) and blocked in 5% skim milk for 1 h. The specific primary antibody was used to incubate with the membrane overnight at 4°C, followed by secondary antibody

incubation for 2 h at room temperature. After Tris Buffered Saline-and Tween-20 (TBST) washing for 1 min, the chemiluminescent substrate kit was used for exposure of the protein band.

Dual-Luciferase Reporter Assay

293T cells were inoculated in 24-well plates. On the next day, cells were co-transfected with WT-lncRNA MIAT/MUT-lncRNA MIAT and miR-29a-5p mimics/NC, respectively. 48 h later, cells were lysed for determining relative luciferase activity (Promega, Madison, WI, USA).

Statistical Analysis

Statistical Product and Service Solutions (SPSS) 22.0 (IBM, Armonk, NY, USA) was used for data analyses. Data were expressed as mean \pm standard deviation. Continuous variables were analyzed by the *t*-test, and categorical variables were analyzed by χ^2 -test or Fisher's exact test. p<0.05 was considered as statistically significant.

Results

Construction of HPH Model in Rats

Rats in normoxia group presented shiny fur, easy breath, normal activities and healthy growth. On the contrary, rats in hypoxia group started to be depressed from the second week. They presented emaciated body shape and shortness of breath. Hemodynamic measurements uncovered that mPAP, RVSP, PASP, and RV/(LV+S) were higher in rats of hypoxia group than those in normoxia group at the end of the first week. These indicators were remarkably elevated in rats of hypoxia group at the second week. Compared with rats undergoing 1-week hypoxia, those suffered 4-week hypoxia exhibited higher mPAP, RVSP, PASP, and RV/(LV+S). These indicators were time-dependently elevated in hypoxia rats (Table I).

Table I. Hemodynamic changes in hypoxic pulmonary hypertension rats (mean±SD).

Group	Normoxia	Hypoxia (1 w)	Hypoxia (2 w)	Hypoxia (4 w)
mPAP (mmHg)	16.00 ± 0.98	17.59 ± 0.65	$21.56 \pm 0.93*$	24.88 ± 0.82*#
RVSP (mmHg)	16.43 ± 0.52	18.41 ± 0.75	$20.84 \pm 0.98*$	23.56 ± 0.53 *#
RASP (mmHg)	21.32 ± 0.52	23.48 ± 0.75	26.56 ± 0.65 *	$30.56 \pm 0.93*$ #
RV/(LV+S)	0.18 ± 0.006	0.21 ± 0.009	0.28 ± 0.007 *	$0.35 \pm 0.014^{*\#}$

Data are expressed as mean±SEM. *p<0.05 vs. Normoxia, *p<0.05 vs. Hypoxia (1 w).



Expression Levels of MIAT and MIR-29a-5p in Lung Tissues of HPH Rats

Compared with normoxia group, MIAT (Figure 1A) was upregulated, while miR-29a-5p (Figure 1B) was downregulated in lung tissues of HPH rats. In addition, activities of ROS (Figure 1C) and MDA (Figure 1D) were remarkably higher in hypoxia group than those in normoxia group. Conversely, activities of T-AOC (Figure 1E), GSH (Figure 1F), CAT (Figure 1G), and SOD (Figure 1H) were lower in hypoxia group.

Hypoxia Upregulated MIAT Expression and Downregulated MiR-29a-5p in HPAECs

An *in vitro* HPH model was constructed in HPAECs undergoing hypoxia for 0, 24, 48, and 72 h. With the prolongation of hypoxia induc-

tion, MIAT (Figure 2A) was time-dependently upregulated, while miR-29a-5p showed the opposite trend (Figure 2B). Protein levels of Nrf2, HO-1, and NQO-1 were downregulated in hypoxia-induced HPAECs compared with those undergoing normoxia treatment (Figure 2C).

Knockdown of MIAT Inhibited Proliferative and Migratory Abilities in Hypoxia-Induced HPAECs

Transfection efficacy of sh-MIAT was tested in hypoxia-induced HPAECs (Figure 3A). Knockdown of MIAT markedly reduced viability (Figure 3B) and migratory cell number (Figure 3C) in HPAECs under hypoxic induction. Moreover, activities of ROS (Figure 3D) and MDA (Figure 3E) were reduced, while T-AOC level (Figure

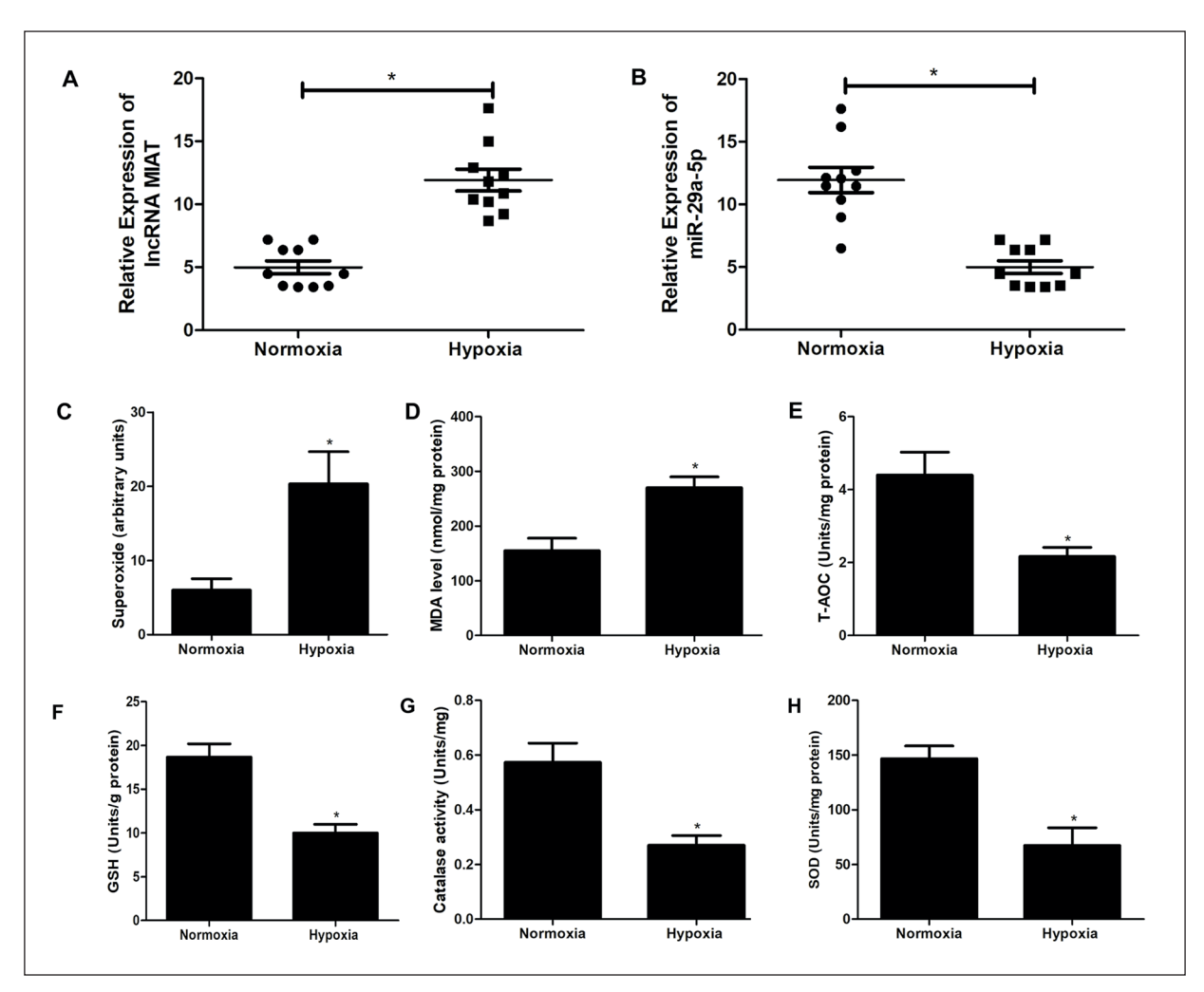


Figure 1. Construction of HPH model in rats. **A, B,** Relative levels of MIAT (**A**) and miR-29a-5p (**B**) in rat lung tissues of normoxia group and hypoxia group. **C-H,** Activities of ROS (**C**), MDA (**D**), T-AOC (**E**), GSH (**F**), CAT (**G**), and SOD (**H**) in rats of normoxia group and hypoxia group. *p<0.05 vs. normoxia group.

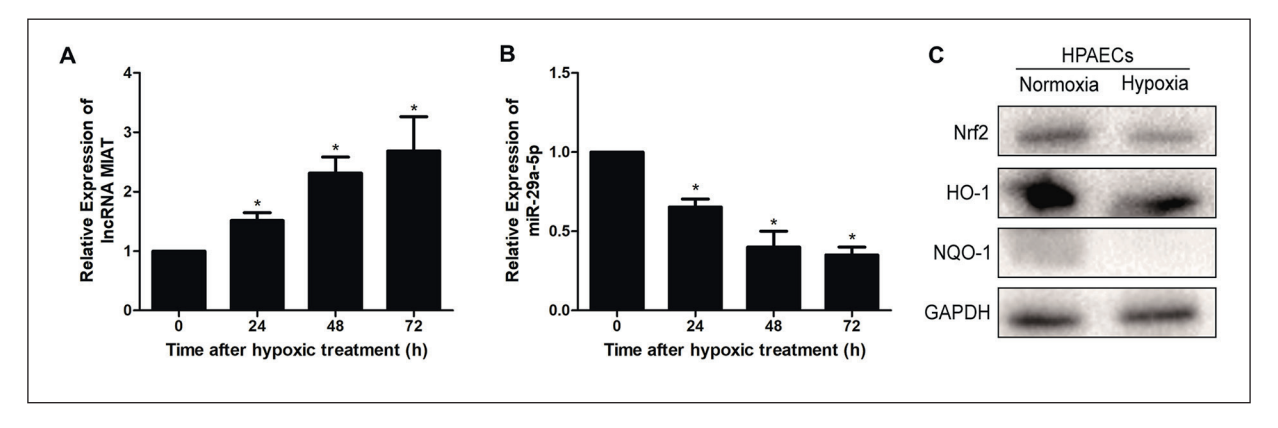


Figure 2. Hypoxia upregulated MIAT expression and downregulated miR-29a-5p in HPAECs. **A, B,** Relative levels of MIAT (**A**) and miR-29a-5p (**B**) in HPAECs undergoing hypoxia for 0, 24, 48, and 72 h. **C,** Protein levels of Nrf2, HO-1, and NQO-1 in HPAECs undergoing normoxia or hypoxia induction. $*p < 0.05 \ vs.$ normoxia group.

3F) was elevated in HAPECs with MIAT knockdown. Under the hypoxic stimulation, transfection of sh-MIAT upregulated protein levels of Nrf2, HO-1, and NQO-1 (Figure 3G). Therefore, MIAT could promote proliferation, migration, oxidative stress, and activate the Nrf2 pathway in hypoxic HPAECs.

MiR-29a-5p Was a Target of LncRNA MIAT

Through bioinformatics analysis, potential binding sequences were discovered in 3'UTR of MIAT and miR-29a-5p (Figure 4A). Subsequently, decreased Luciferase activity in 293T cells co-transfected with miR-29a-5p mimics and

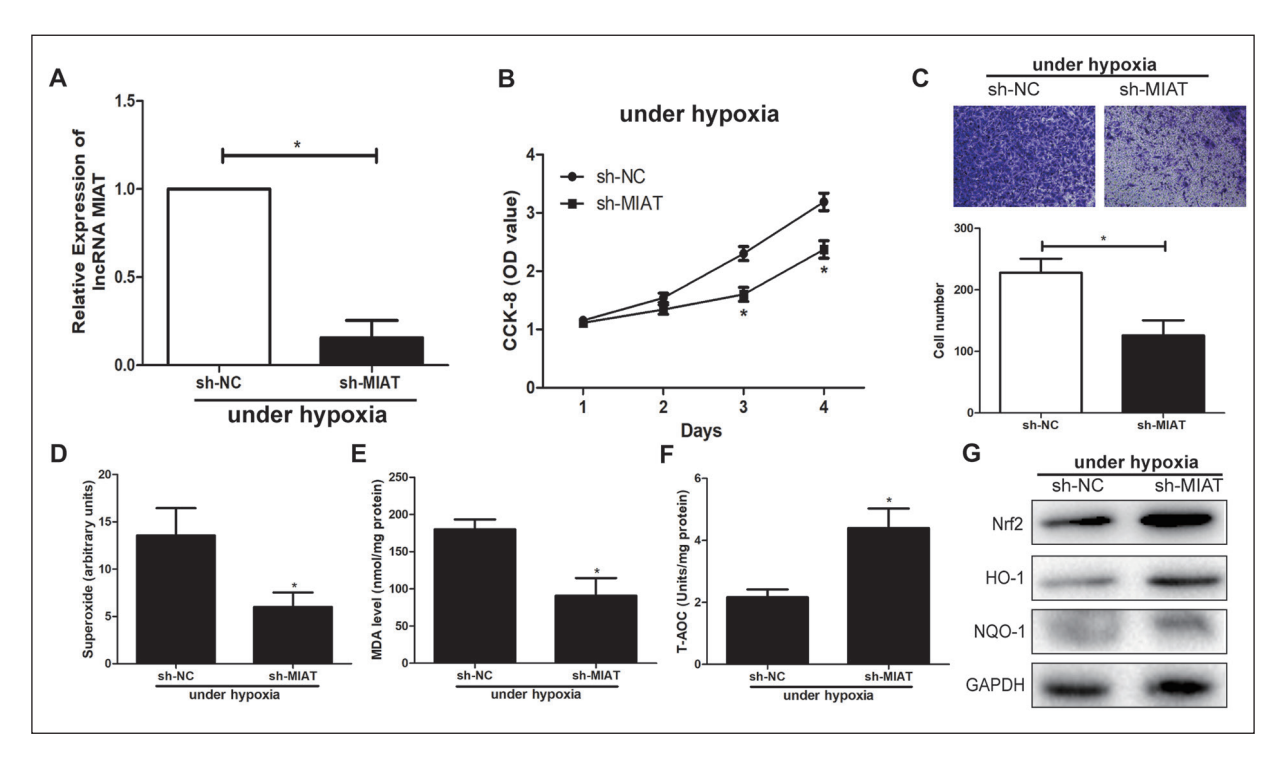


Figure 3. Knockdown of MIAT inhibited proliferative and migratory abilities in hypoxia-induced HPAECs. MIAT level (**A**), viability (**B**), migratory cell number (**C**) (magnification: $20 \times$), ROS level (**D**), MDA level (**E**), T-AOC level (**F**) and protein levels of Nrf2, HO-1 and NQO-1 (**G**) in hypoxia-induced HPAECs transfected with sh-NC or sh-MIAT. * $p < 0.05 \ vs.$ sh-NC group.

9026

WT-lncRNA MIAT verified that miR-29a-5p was the target binding MIAT (Figure 4B). Transfection of sh-MIAT downregulated miR-29a-5p level in HAPECs (Figure 4C). Besides, a negative correlation was identified between expression levels of MIAT and miR-29a-5p (Figure 4D).

Knockdown of MiR-29a-5p Partially Alleviated the Effects of MIAT on Proliferative and Migratory Abilities in Hypoxia-Induced HPAECs

To determine the involvement of miR-29a-5p in MIAT-regulated phenotypes of HPAECs, transfection efficacy of miR-29a-5p inhibitor was firstly tested (Figure 5A). Of note, inhibited viability (Figure 5B) and migration (Figure 5C) in hypoxia-induced HPAECs with MIAT knockdown were partially alleviated by co-transfection of miR-29a-5p inhibitor. Similarly, regulatory effects of MIAT on activities of ROS (Figure 5D), MDA (Figure 5E), and T-AOC (Figure 5F) in hypoxia-induced HPAECs were reversed by knockdown of miR-29a-5p.

Discussion

HPH is a progressive pathological state, which is the key event in pulmonary heart disease. Currently,

there is no curable treatment for HPH. Conventional drugs applied for dilating the pulmonary artery can improve pulmonary hypertension in the short term. Nevertheless, long-term application of pulmonary artery dilation drugs may even aggravate hypoxia¹⁻³. Effective therapeutic strategies for HPH urgently need to be solved^{4,5}. Hypoxia is the initial factor for pulmonary hypertension, which directly or indirectly damages structure and function of the pulmonary artery³⁻⁵. The occurrence of HPH is an adaptive process of pulmonary vascular cells and interstitial spontaneous hypoxic environment. Pulmonary vascular remodeling is a re-adjustment of pulmonary vessels under hypoxia, leading to alterations on its structure, function, and metabolism⁴⁻⁶. Detection of abnormally expressed genes during the development of HPH provides a theoretical basis and research direction for clinical treatment of HPH^{7,8}.

In recent years, lncRNAs have been well concerned because of their vital functions in human diseases¹²⁻¹⁴. Compared with protein-encoding genes, the abundances of lncRNAs are relatively low^{15,16}. However, their conserved sequences and secondary structure highlight the time- and space-specificity¹⁶⁻¹⁸. A great number of lncRNAs have been identified in regulating cardiovascular diseases^{18,19}. By mediating vascular functions, lncRNAs could participate in the development of HPH¹⁸. In this paper, MIAT was upregulated

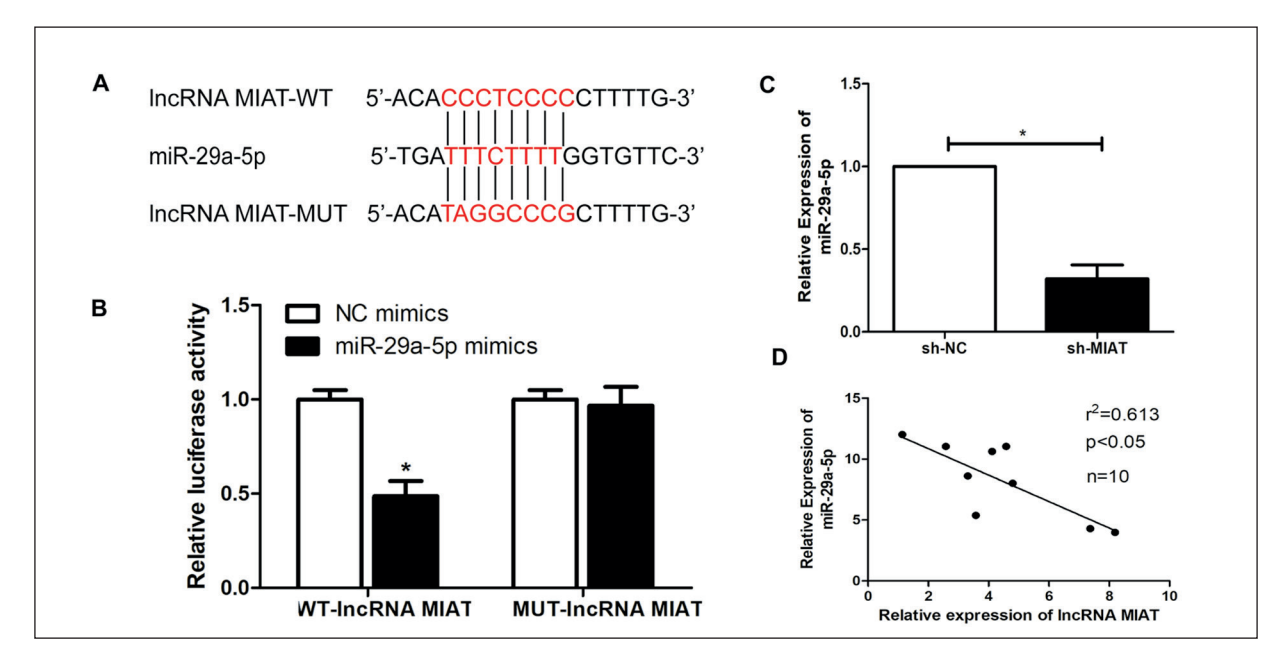


Figure 4. MiR-29a-5p was a target of lncRNA MIAT. **A,** Binding sequences in 3'UTR of MIAT and miR-29a-5p. **B,** Luciferase activity in 293T cells co-transfected with NC/miR-29a-5p mimics and WT-lncRNA MIAT/MUT-lncRNA MIAT. **C,** MiR-29a-5p level in hypoxia-induced HPAECs transfected with sh-NC or sh-MIAT. **D,** Negative correlation between expression levels of MIAT and miR-29a-5p.

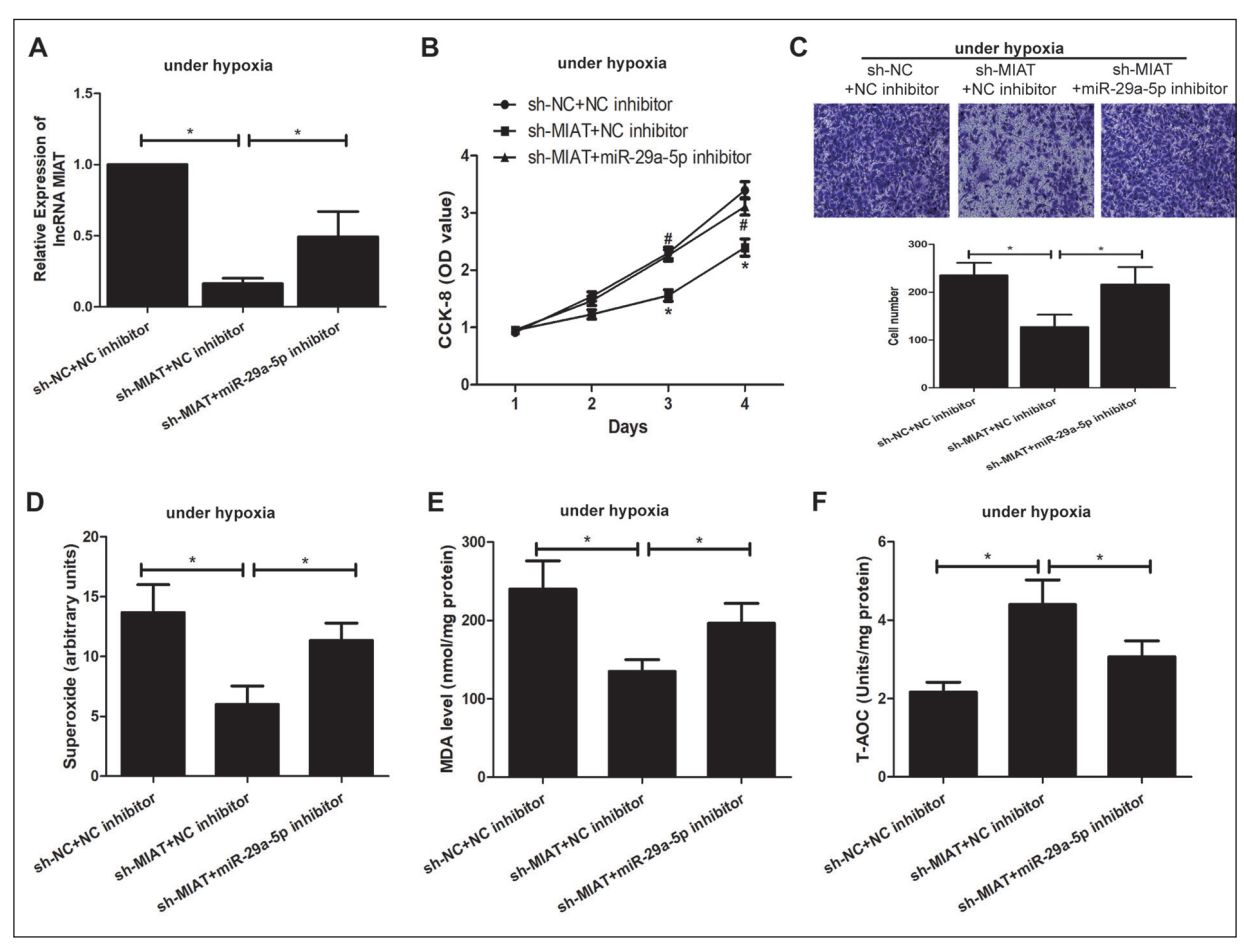


Figure 5. Knockdown of miR-29a-5p partially alleviated the effects of MIAT on proliferative and migratory abilities in hypoxia-induced HPAECs. MiR-29a-5p level (**A**), viability (**B**), migratory cell number (**C**) (magnification: $20\times$), ROS level (**D**), MDA level (**E**) and T-AOC level (**F**) in hypoxia-induced HPAECs transfected with sh-NC+NC, sh-MIAT+NC or sh-MIAT+miR-29a-5p inhibitor. *p<0.05 vs. sh-NC group.

in both hypoxia-induced rat lung tissues and hypoxia-induced HPAECs, while miR-29a-5p was downregulated. Subsequently, knockdown of MI-AT markedly suppressed proliferative and migratory abilities in hypoxia-induced HPAECs. In addition, previous studies^{20,21} have found that overproduction of reactive oxygen caused dysfunction of organelles, which induced hypoxic pulmonary hypertension. Furthermore, several researches^{21,22} have illustrated that oxidant stress activates a specific downstream signaling pathway, which contributes to activating Nrf2 pathway. So, in this study, oxidative stress indicators, such as ROS and MDA were significantly increased in the hypoxic pulmonary hypertension model. However, antioxidant index, including T-AOC, GSH, CAT, and SOD significantly decreased under the hypoxia induction, and knockdown of MIAT could markedly protect against oxidative stress in the hypoxic pulmonary hypertension.

LncRNA-miRNA interaction is critical in regulating disease progression^{23,24}. By recognizing and binding 3'UTR of the target miRNA, lncRNA could degrade or inhibit its translation^{25,26}. Here, we have verified that miR-29a-5p was the target gene binding MIAT. MiR-29a-5p is reported to regulate biological functions of its downstream genes²⁷. Our findings uncovered that knockdown of miR-29a-5p could partially relieve the oxidative stress state of silenced MIAT on hypoxia-induced HPAECs. Therefore, as a novel lncRNA, MIAT could aggravate oxidative stress in the hypoxic pulmonary hypertension model by sponging miR-29a-5p and inhibiting Nrf2 pathway.

Conclusions

MIAT promotes proliferative and migratory abilities in hypoxia-induced HPAECs by targeting miR-29a-5p, thus aggravating the development of HPH.

Conflict of Interest

The Authors declare that they have no conflict of interests.

References

- ROWAN SC, KEANE MP, GAINE S, McLOUGHLIN P. Hypoxic pulmonary hypertension in chronic lung diseases: novel vasoconstrictor pathways. Lancet Respir Med 2016; 4: 225-236.
- FULORIA M, ASCHNER JL. Persistent pulmonary hypertension of the newborn. Semin Fetal Neonatal Med 2017; 22: 220-226.
- LEHNER A, SCHULZE-NEICK I, FISCHER M, FERNANDEZ-RODRI-GUEZ S, ULRICH S, HAAS NA, JAKOB A. The creation of an interatrial right-to-left shunt in patients with severe, irreversible pulmonary hypertension: rationale, devices, outcomes. Curr Cardiol Rep 2019; 21: 31.
- 4) OLSCHEWSKI A, BERGHAUSEN EM, EICHSTAEDT CA, FLEIS-CHMANN BK, GRUNIG E, GRUNIG G, HANSMANN G, HAR-BAUM L, HENNIGS JK, JONIGK D, KUBLER WM, KWAPISZE-WSKA G, PULLAMSETTI SS, STACHER E, WEISSMANN N, WEN-ZEL D, SCHERMULY RT. [Pathobiology, pathology and genetics of pulmonary hypertension: recommendations of the Cologne Consensus Conference 2016]. Dtsch Med Wochenschr 2016; 141: S4-S9.
- DUNHAM-SNARY KJ, Wu D, SYKES EA, THAKRAR A, PARLOW L, MEWBURN JD, PARLOW JL, ARCHER SL. Hypoxic pulmonary vasoconstriction: from molecular mechanisms to medicine. Chest 2017; 151: 181-192.
- Huetsch J, Shimoda LA. Na(+)/H(+) exchange and hypoxic pulmonary hypertension. Pulm Circ 2015; 5: 228-243.
- BONNET S, ARCHER SL. Potassium channel diversity in the pulmonary arteries and pulmonary veins: implications for regulation of the pulmonary vasculature in health and during pulmonary hypertension. Pharmacol Ther 2007; 115: 56-69.
- MICHELAKIS ED, THEBAUD B, WEIR EK, ARCHER SL. Hypoxic pulmonary vasoconstriction: redox regulation of O2-sensitive K+ channels by a mitochondrial O2-sensor in resistance artery smooth muscle cells. J Mol Cell Cardiol 2004; 37: 1119-1136.
- WANG J, ZHU S, MENG N, HE Y, LU R, YAN GR. ncRNA-encoded peptides or proteins and cancer. Mol Ther 2019; 27: 1718-1725.
- NING B, YU D, YU AM. Advances and challenges in studying noncoding RNA regulation of drug metabolism and development of RNA therapeutics. Biochem Pharmacol 2019; 169: 113638.
- KARALI M, BANFI S. Non-coding RNAs in retinal development and function. Hum Genet 2019; 138: 957-971.
- CAO M, ZHAO J, Hu G. Genome-wide methods for investigating long noncoding RNAs. Biomed Pharmacother 2019; 111: 395-401.
- LIN R, TURECKI G. Noncoding RNAs in depression. Adv Exp Med Biol 2017; 978: 197-210.
- 14) ALISHAHI M, GHAEDRAHMATI F, KOLAGAR TA, WINLOW W, NIKKAR N, FARZANEH M, KHOSHNAM SE. Long non-coding RNAs and cell death following ischemic stroke. Metab Brain Dis 2019; 34: 1243-1251.

- 15) FANG F, ZHANG K, CHEN Z, WU B. Noncoding RNAs: new insights into the odontogenic differentiation of dental tissue-derived mesenchymal stem cells. Stem Cell Res Ther 2019; 10: 297.
- FERRE F, COLANTONI A, HELMER-CITTERICH M. Revealing protein-IncRNA interaction. Brief Bioinform 2016; 17: 106-116.
- 17) RAMNARINE VR, KOBELEV M, GIBB EA, NOURI M, LIN D, WANG Y, BUTTYAN R, DAVICIONI E, ZOUBEIDI A, COLLINS CC. The evolution of long noncoding RNA acceptance in prostate cancer initiation, progression, and its clinical utility in disease management. Eur Urol 2019; 76: 546-559.
- 18) YAN B, YAO J, LIU JY, LI XM, WANG XO, LI YJ, TAO ZF, SONG YC, CHEN Q, JIANG Q. IncRNA-MIAT regulates microvascular dysfunction by functioning as a competing endogenous RNA. Circ Res 2015; 116: 1143-1156.
- 19) ZHOU H, WANG B, YANG YX, JIA QJ, ZHANG A, QI ZW, ZHANG JP. Long noncoding RNAs in pathological cardiac remodeling: a review of the update literature. Biomed Res Int 2019; 2019: 7159592.
- 20) SIQUEIRA R, COLOMBO R, CONZATTI A, DE CASTRO AL, CARRARO CC, TAVARES AMV, FERNANDES TRG, ARAUJO ASDR, BELLÓ-KLEIN A. Effects of ovariectomy on antioxidant defence systems in the right ventricle of female rats with pulmonary arterial hypertension induced by monocrotaline. Can J Physiol Pharmacol 2018; 96: 295-303.
- 21) MURALIDHARAN P, HAYES D JR, BLACK SM, MANSOUR HM. microparticulate/nanoparticulate powders of a novel nrf2 activator and an aerosol performance enhancer for pulmonary delivery targeting the lung Nrf2/Keap-1 pathway. Mol Syst Des Eng 2016; 1: 48-65.
- 22) VOELKEL NF, BOGAARD HJ, AL HUSSEINI A, FARKAS L, GOMEZ-ARROYO J, NATARAJAN R. Antioxidants for the treatment of patients with severe angioproliferative pulmonary hypertension? Antioxid Redox Signal 2013; 18: 1810-7.
- Dahariya S, Paddibhatla I, Kumar S, Raghuwanshi S, Pallepati A, Gutti RK. Long non-coding RNA: Classification, biogenesis and functions in blood cells. Mol Immunol 2019; 112: 82-92.
- 24) BASAVAPPA M, CHERRY S, HENAO-MEJIA J. Long noncoding RNAs and the regulation of innate immunity and host-virus interactions. J Leukoc Biol 2019; 106: 83-93.
- PARASKEVOPOULOU MD, HATZIGEORGIOU AG. Analyzing miRNA-LncRNA interactions. Methods Mol Biol 2016; 1402: 271-286.
- 26) BALLANTYNE MD, McDonald RA, BAKER AH. IncRNA/ MicroRNA interactions in the vasculature. Clin Pharmacol Ther 2016; 99: 494-501.
- 27) RAGNI E, PERUCCA OC, DE LUCA P, VIGANO M, COLOMBINI A, LUGANO G, BOLLATI V, DE GIROLAMO L. MiR-22-5p and miR-29a-5p are reliable reference genes for analyzing extracellular vesicle-associated miRNAs in adipose-derived mesenchymal stem cells and are stable under inflammatory priming mimicking osteoarthritis condition. Stem Cell Rev Rep 2019; 15: 743-754.